Amplitude death in oscillators coupled by asymmetric connection delays with tree graph topology

EPJ manuscript No.
(will be inserted by the editor)

Amplitude death in oscillators coupled by asymmetric connection delays with tree graph topology

Y. Okigawa[1], Y. Sugitani[1a], and K. Konishi[2]

[1] Department of Electrical and Electronic Engineering, Ibaraki University
4-12-1 Nakanarusawa, Hitachi, Ibaraki 316-8511, Japan
[2] Department of Electrical and Information Systems, Osaka Prefecture University
1-1 Gakuen-cho, Naka-ku, Sakai, Osaka 599-8531, Japan

Received: date / Revised version: date

Abstract. The present study investigates amplitude death in an oscillator network with *asymmetric* connection delays and a tree graph topology. A frequency domain analysis reveals that the local steady-state stability is dominated by the sum of the connection delays between connected oscillators. Based on this observation, we show that the local steady-state stability can be reduced to that with symmetric connection delays, as long as the sum of the connection delays between connected oscillators satisfies a certain condition. Numerical simulations verify the analytical results.

PACS. XX.XX.XX No PACS code given

1 Introduction

Mutual interactions among oscillators cause two major oscillation quenching phenomena: oscillation death (OD) and amplitude death (AD) [1–3]. Oscillation death is the emergence of a stable heterogeneous steady state by interactions, whereas AD is the stabilization of a homogeneous steady state in coupled oscillators. Since AD can eliminate unwanted oscillations in many practical systems, it has been actively investigated not only from an academic perspective [4–18], but also from an engineering point of view [19–24].

The connection delay in the interactions plays a crucial role in the occurrence of AD [25]. Since connection delay is inherent in real-world networks, AD in delayed-coupled oscillators has been intensively investigated both analytically and experimentally [5–12,16–18,20–23]. Most studies on AD consider only *symmetric* connection delays: $\tau_{ij} = \tau_{ji}$ holds for any i and j, where τ_{ij} is the connection delay from oscillator j to oscillator i (see Fig. 1). In real-world networks, however, such as neural networks [26], the connection delays are usually not symmetric, and are instead *asymmetric* (i.e., $\tau_{ij} \neq \tau_{ji}$).

To the best of our knowledge, there have been few efforts to deal with AD induced with asymmetric connection delays, because such delays complicate the analytical treatment of the stability. Amplitude death induced with asymmetric connection delays has been numerically observed [26,27]. Although these studies [26,27] confirm the occurrence of AD in various network topologies, they do not provide a sufficient analytical discussion. A previous study [28] considered two oscillators with recurrent coupling of asymmetric connection delays (i.e., $\tau_{12} \neq \tau_{21}$), and reported analytical results showing that the stability of the steady state depends on the sum of the connection delays (i.e., $\tau_{12}+\tau_{21}$). However, it is difficult to extend the results of this previous study [28] to more general network topologies.

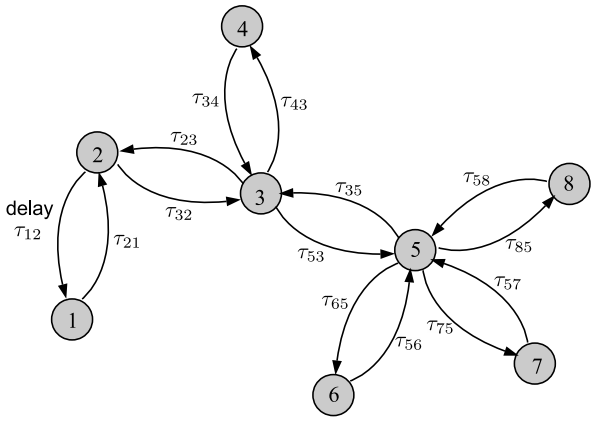

Fig. 1. Example of asymmetric delayed-coupled oscillators with a tree graph topology ($N = 8$).

The goal of the present study is to show that the analytical results [28] with asymmetric connection delays can be extended to networks if their topology is restricted to a tree graph. In the tree graph, the stability of steady state depends on the sum of the connection delays $\tau_{ij} + \tau_{ji}$ be-

[a] e-mail: yoshiki.sugitani.0301@vc.ibaraki.ac.jp

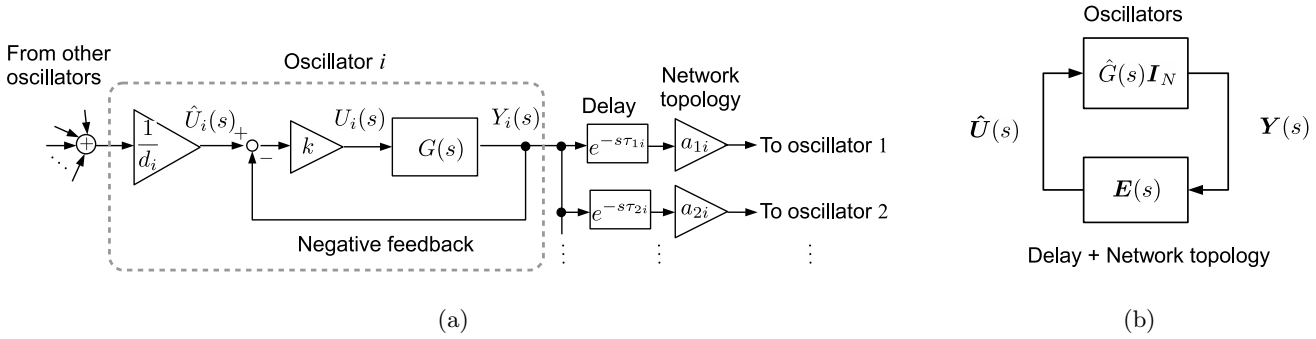

Fig. 2. Block diagrams of linear system given by Eqs. (4) and (5): (a) oscillator i, (b) entire system.

tween connected oscillators. This allows us to prove that the stability of the steady state with asymmetric connection delays is reduced to that with symmetric connection delays if the network topology is a tree graph and the sums of the connection delays, τ_{ij} and τ_{ji}, are identical for any combination of i and j. The analytical results are numerically confirmed through examples.

2 Mathematical model

This section introduces asymmetric delayed-coupled oscillators with a tree graph topology, and investigates the stability of the steady state by linear stability analysis based on frequency domain analysis.

2.1 Delayed-coupled oscillators

We herein consider N delayed-coupled identical oscillators (see Fig. 1):

$$\begin{aligned} \dot{\boldsymbol{x}}_i(t) &= \boldsymbol{F}(\boldsymbol{x}_i(t)) + \boldsymbol{b}u_i(t), \\ y_i(t) &= \boldsymbol{c}\boldsymbol{x}_i(t), \end{aligned} \tag{1}$$

where $\boldsymbol{x}_i(t) \in \mathbb{R}^{m\times 1}$ is the state variable of oscillator $i \in \{1,\dots,N\}$ at time $t \geq 0$. The nonlinear function $\boldsymbol{F}:\mathbb{R}^{m\times 1}\to\mathbb{R}^{m\times 1}$ of each oscillator is assumed to have at least one equilibrium point $\boldsymbol{x}^*:\boldsymbol{0}=\boldsymbol{F}(\boldsymbol{x}^*)$. The vectors $\boldsymbol{b}\in\mathbb{R}^{m\times 1}$ and $\boldsymbol{c}\in\mathbb{R}^{1\times m}$ are the input and output coefficient vectors, respectively. Here, $y_i(t)\in\mathbb{R}$ is the output signal of oscillator i. The input signal $u_i(t)\in\mathbb{R}$ is given by

$$u_i(t) = k\left\{\left(\frac{1}{d_i}\sum_{j=1}^{N} a_{ij}y_j(t-\tau_{ij})\right) - y_i(t)\right\}, \tag{2}$$

where $k\in\mathbb{R}$ denotes the coupling strength, $y_j(t-\tau_{ij})$ is the delayed output signal from oscillator j, and τ_{ij} denotes the connection delay from oscillator j to oscillator i.

The network topology is governed by the adjacency matrix $\{\boldsymbol{A}\}_{ij} := a_{ij}$ as follows. Oscillators i and j are connected if $a_{ij}=a_{ji}=1$, otherwise $a_{ij}=a_{ji}=0$. There is no self-delayed feedback, i.e., $a_{ii}=0$. The degree of oscillator i is defined as $d_i := \sum_{j=1}^{N} a_{ij}$. Equation (2) describes a diffusive coupling[1]. In Eq. (2), there is a negative feedback term, and the delayed signal is divided by the degree d_i so that the input signal $u_i(t)$ becomes zero when $y_j(t-\tau_{ij}) = \boldsymbol{c}\boldsymbol{x}^*$ and $y_i(t)=\boldsymbol{c}\boldsymbol{x}^*$, $\forall i,j$. The network is assumed to have a tree graph topology (see, e.g., Fig. 1) [31], which is connected, acyclic, and undirected. In tree graphs, there exists a unique path between every two oscillators. The network has N nodes and $(N-1)$ edges, i.e., $\sum_{i=1}^{N}\sum_{j=i}^{N} a_{ij} = N-1$.

Coupled oscillators (1) and (2) have the following homogeneous steady state:

$$\left[\boldsymbol{x}_1^T(t)\cdots\boldsymbol{x}_N^T(t)\right]^T = \left[\boldsymbol{x}^{*T}\cdots\boldsymbol{x}^{*T}\right]^T. \tag{3}$$

Note that AD is a phenomenon in which oscillator state variables converge to a homogeneous steady state[2]. Throughout the present paper, we analyze the local stability of steady state (3). Linearizing Eqs. (1) and (2) in steady state (3) yields

$$\begin{aligned} \Delta\dot{\boldsymbol{x}}_i(t) &= \boldsymbol{J}\Delta\boldsymbol{x}_i(t) + \boldsymbol{b}\Delta u_i(t), \\ \Delta y_i(t) &= \boldsymbol{c}\Delta\boldsymbol{x}_i(t), \end{aligned} \tag{4}$$

where $\Delta\boldsymbol{x}_i(t) := \boldsymbol{x}_i(t)-\boldsymbol{x}^*$, $\boldsymbol{J} := \{\mathrm{d}\boldsymbol{F}(\boldsymbol{x})/\mathrm{d}\boldsymbol{x}\}_{\boldsymbol{x}=\boldsymbol{x}^*}$, and

$$\Delta u_i(t) = k\left\{\left(\frac{1}{d_i}\sum_{j=1}^{N} a_{ij}\Delta y_j(t-\tau_{ij})\right) - \Delta y_i(t)\right\}. \tag{5}$$

Steady state (3) is stable if and only if the linearized system given by Eqs. (4) and (5) is stable.

[1] This type of diffusive coupling is used in many previous studies [8,21,26,29,30].

[2] The stabilization of the homogeneous steady state is not sufficient, but is necessary for AD to be induced, because AD does not occur when the initial state variables are located outside the basin of attraction for the stabilized homogeneous steady state.

2.2 Frequency domain analysis

We consider the stability of the linearized system given by Eqs. (4) and (5) based on a frequency domain analysis. Let $\mathcal{L}[\cdot]$ be the Laplace transform operator. By applying the Laplace transform to both sides of Eq. (4), we obtain the transfer function of oscillator i in steady state (3), which relates the input signal $U_i(s) := \mathcal{L}[\Delta u_i(t)]$ to the output signal $Y_i(s) := \mathcal{L}[\Delta y_i(t)]$ as follows:

$$G(s) := \frac{Y_i(s)}{U_i(s)} = \boldsymbol{c}\left(s\boldsymbol{I}_m - \boldsymbol{J}\right)^{-1}\boldsymbol{b}, \tag{6}$$

where $\boldsymbol{I}_m$ is an $m \times m$ identity matrix. The Laplace transform of Eq. (5) is expressed as

$$U_i(s) = k\left(\hat{U}_i(s) - Y_i(s)\right), \tag{7}$$

where

$$\hat{U}_i(s) := \frac{1}{d_i}\sum_{j=1}^{N} a_{ij} Y_j(s) e^{-s\tau_{ij}}, \tag{8}$$

is the Laplace transform of the delayed signals from the other oscillators. From Eqs. (6)-(8), the linear system given by Eqs. (4) and (5) can be described by the block diagram shown in Fig. 2(a). Considering the negative feedback loop in Fig. 2(a), the output signal $Y_i(s)$ can be written as

$$Y_i(s) = \hat{G}(s)\hat{U}_i(s), \tag{9}$$

where $\hat{G}(s) := kG(s)/(1 + kG(s))$ is the transfer function that includes the negative feedback term in Eq. (7). Taking all oscillators into account, Eqs. (8) and (9) can be respectively rewritten as

$$\hat{\boldsymbol{U}}(s) = \boldsymbol{E}(s)\boldsymbol{Y}(s), \tag{10}$$

$$\boldsymbol{Y}(s) = \hat{G}(s)\hat{\boldsymbol{U}}(s), \tag{11}$$

where $\hat{\boldsymbol{U}}(s) := \left[\hat{U}_1(s)\cdots\hat{U}_N(s)\right]^T$, $\boldsymbol{Y}(s) := \left[Y_1(s)\cdots Y_N(s)\right]^T$, and

$$\boldsymbol{E}(s) := \begin{bmatrix} 0 & \frac{a_{12}}{d_1}e^{-s\tau_{12}} & \cdots & \frac{a_{1N}}{d_1}e^{-s\tau_{1N}} \\ \frac{a_{21}}{d_2}e^{-s\tau_{21}} & \ddots & \ddots & \vdots \\ \vdots & \ddots & \ddots & \frac{a_{(N-1)N}}{d_{N-1}}e^{-s\tau_{(N-1)N}} \\ \frac{a_{N1}}{d_N}e^{-s\tau_{N1}} & \cdots & \frac{a_{N(N-1)}}{d_N}e^{-s\tau_{N(N-1)}} & 0 \end{bmatrix}. \tag{12}$$

Equations (10) and (11) indicate that the entire system of Eqs. (4) and (5) can be expressed by the closed-loop system shown in Fig. 2(b). The stability of this closed-loop system is governed by the roots of the following characteristic function[3]:

$$g(s) = \left\{D_g(s) + kN_g(s)\right\}\hat{g}(s), \tag{13}$$

where $D_g(s) := \det\left(s\boldsymbol{I}_m - \boldsymbol{J}\right)$, $N_g(s) := \boldsymbol{c}\,\mathrm{adj}\left(s\boldsymbol{I}_m - \boldsymbol{J}\right)\boldsymbol{b}$, and

$$\hat{g}(s) := \det\left[\boldsymbol{I}_N - \hat{G}(s)\boldsymbol{E}(s)\right]. \tag{14}$$

As a consequence, steady state (3) is stable (i.e., AD occurs) if and only if $g(s)$ is stable. In general, however, the stability analysis of $g(s)$ is difficult due to asymmetric connection delays. Note that if the connection delays are symmetric and identical, $\tau_{ij} = \tau_{ji} \equiv \tau, \forall i, j$, then matrix $\boldsymbol{E}(s)$ in $\hat{g}(s)$ can be expressed as $\boldsymbol{E}(s) = \boldsymbol{D}^{-1}\boldsymbol{A}e^{-s\tau}$ with adjacency matrix $\boldsymbol{A}$ and $\boldsymbol{D} := \mathrm{diag}(d_1, \ldots, d_N)$. Since matrix $\boldsymbol{D}^{-1}\boldsymbol{A}$ is known to be diagonalizable [29], $g(s)$ can be separated into simple characteristic quasi-polynomials, i.e., we can easily analyze its stability.

For asymmetric connection delays, we cannot separate $g(s)$. Instead of diagonalization of the matrix, we use a feature of the tree graph and derive an important fact about the stability of steady state (3).

Lemma 1 *Consider the oscillator network given by Eqs. (1) and (2) with a tree graph. The stability of steady state (3) depends only on the sum of the connection delays, $\tau_{ij} + \tau_{ji}$, for all combinations of (i, j) satisfying $a_{ij} = 1$.*

Proof The proof will use a feature of the tree graph. See Appendix A for more details. □

Lemma 1 indicates that the sum of the connection delays between connected oscillators affects the stability of steady state (3). We now provide an example for Lemma 1. Figure 3 depicts the two networks with different connection delays, i.e., (a) asymmetric connection delays and (b) symmetric connection delays. Although the connection delays are different, both networks have the same sum of connection delays $\tau_{12} + \tau_{21} = 2$ and $\tau_{13} + \tau_{31} = 2$. According to Lemma 1, we can say that the networks have the same stability of steady state (3). This relation between asymmetric and symmetric connection delays can be summarized as the following main theorem.

Theorem 1 *The stability of steady state (3) in a network given by Eqs. (1) and (2) with asymmetric connection delays is equal to that in the network given by Eqs. (1) and (2) with symmetric connection delays $\tau_{ij} \equiv \tau, \forall i, j$, if the network topology is a tree graph and asymmetric connection delays satisfy*

$$\tau_{ij} + \tau_{ji} = 2\tau, \forall (i,j) \in \left\{(i,j) \,|\, i, j \in \{1, \ldots, N\},\, a_{ij} = 1\right\}. \tag{15}$$

Proof This is obvious from Lemma 1. The proof is omitted. □

Theorem 1 indicates that the stability of steady state (3) in an oscillator network coupled by asymmetric connection delays can be reduced to that in an oscillator network coupled by symmetric connection delays if the network topology is a tree graph and the sums of the connection delays, τ_{ij} and τ_{ji}, between any connected oscillators i and j are identical.

[3] The characteristic function is obtained by adding an additional input to the signal $\hat{\boldsymbol{U}}(s)$ in the block diagram of Fig. 2(b) and deriving the transfer function from the additional input to the output $\boldsymbol{Y}(s)$.

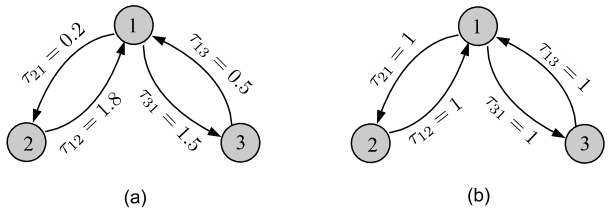

Fig. 3. An example of two networks with a tree graph topology, which has the same stability of steady state (3): (a) asymmetric delayed-coupled network, (b) symmetric delayed-coupled network.

Furthermore, Theorem 1 can be considered as an extension of the result reported in a previous study [28], which showed that, for a pair of oscillators (i.e., $N = 2$), the stability of steady state (3) depends only on $\tau_{12} + \tau_{21}$.

3 Numerical examples

The validity of Theorem 1 is confirmed through numerical examples. We use Rössler oscillators, which are expressed by Eq. (1) as

$$\boldsymbol{F}(\boldsymbol{x}) = \begin{bmatrix} -x^{(2)} - x^{(3)} \\ x^{(1)} + ax^{(2)} \\ b + x^{(3)}\left(x^{(1)} - c\right) \end{bmatrix}, \quad \boldsymbol{b} = \begin{bmatrix} 1 \\ 0 \\ 0 \end{bmatrix}, \quad \boldsymbol{c} = \begin{bmatrix} 1 \\ 0 \\ 0 \end{bmatrix}^T, \tag{16}$$

where the parameters are set to $a = 0.2$, $b = 0.2$, and $c = 5.7$. The Rössler oscillator has the two equilibrium points:

$$\boldsymbol{x}^*_{\pm} := \left[x^{(1)*}_{\pm},\ x^{(2)*}_{\pm},\ x^{(3)*}_{\pm}\right]^T = \left[aP_{\pm},\ -P_{\pm},\ P_{\pm}\right]^T, \tag{17}$$

where $P_{\pm} := \left(c \pm \sqrt{c^2 - 4ab}\right)/(2a)$. Since $\boldsymbol{x}^*_+$ satisfies the odd number property [30], we only consider the stability of $\boldsymbol{x}^*_-$.

3.1 Tree graph

Let us consider the tree graph topology illustrated in Fig. 1. First, we analyze the stability for symmetric and identical connection delays $\tau_{ij} \equiv \tau, \forall i, j$. The stability region on the connection parameter (k, τ) space is shown in Fig. 4(a). The curves denote a solution of $g(\mathrm{i}\lambda) = 0$ with $\mathrm{i} := \sqrt{-1}$ and $\lambda \in \mathbb{R}$. When the parameter set (k, τ) crosses the thick (thin) curves as k increases, then a pair of roots for $g(s) = 0$ traverse the imaginary axis from right to left (from left to right). All of the roots of $g(s) = 0$ have a negative real part when the parameter set (k, τ) is in the stability region.

We now focus on a connection delay $\tau = \tau^* := 1.8$ as an example, which is illustrated by the red dotted line in Fig. 4(a)[4]. Let us consider asymmetric connection delays

[4] The validity of Theorem 1 has been also numerically confirmed using other connection delay τ^* values.

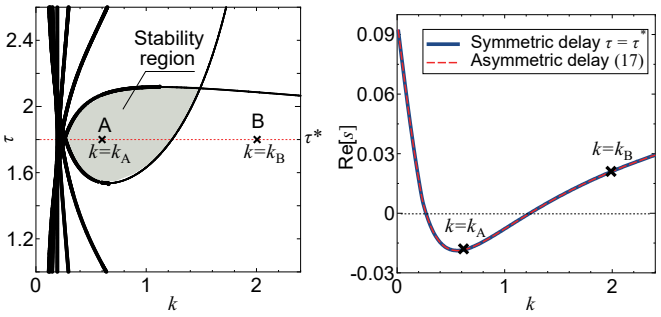

(a) Stability region for symmetric delay

(b) Largest real part of the root of $g(s) = 0$

Fig. 4. Stability region and the largest real part of roots of $g(s) = 0$ for delayed-coupled Rössler oscillators, the topology of which is illustrated in Fig. 1.

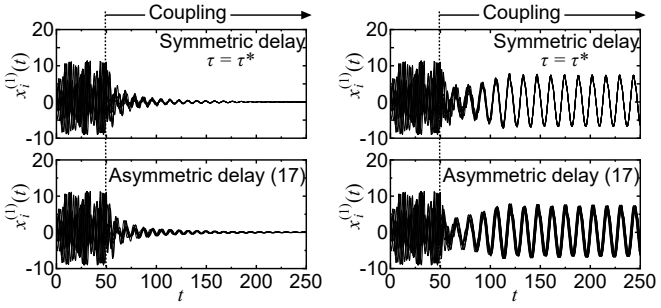

(a) $k = k_A$

(b) $k = k_B$

Fig. 5. Time-series data for delayed-coupled Rössler oscillators at (a) $k = k_A$ and (b) $k = k_B$. Both of the upper sides denote symmetric connection delays $\tau = \tau^*$, which correspond to points A and B in Fig. 4(a), while the lower sides denote the asymmetric connection delays (18).

satisfying Eq. (15) with $\tau = \tau^*$, i.e., $\tau_{ij} + \tau_{ji} = 2\tau^* = 3.6$, $\forall i, j$, as follows:

$$\boldsymbol{T} = \begin{pmatrix} * & 0.2 & * & * & * & * & * & * \\ 3.4 & * & 3.2 & * & * & * & * & * \\ * & 0.4 & * & 1.3 & 0.6 & * & * & * \\ * & * & 2.3 & * & * & * & * & * \\ * & * & 3.0 & * & * & 3.5 & 1.5 & 1.8 \\ * & * & * & * & 0.1 & * & * & * \\ * & * & * & * & 2.1 & * & * & * \\ * & * & * & * & 1.8 & * & * & * \end{pmatrix}, \tag{18}$$

where $\{\boldsymbol{T}\}_{ij} := \tau_{ij}$. Here, the symbol $*$ denotes no connection. According to Theorem 1, delayed-coupled oscillators with asymmetric connection delays (18) have the same stability of steady state (3) as those with symmetric connection delays of $\tau = \tau^* := 1.8$.

In order to confirm this, the largest real part of roots of $g(s) = 0$ for symmetric (blue solid line) and asymmetric (red dotted line) connection delays with varying

coupling strength k is shown in Fig. 4(b). We can see that symmetric and asymmetric connection delays have the same largest real part. In particular, for both connection delays, the largest real part is negative in the range of $k \in (0.27, 1.23)$, which agrees well with the red dotted line in Fig. 4(a). Therefore, from Fig. 4(b), we can confirm that the stability of steady state (3) with symmetric connection delays $\tau = \tau^*$ is equivalent to that with asymmetric connection delays (18) satisfying relation (15).

Figures 5(a) and 5(b) show the time-series data of the first variables $x_i^{(1)}(t)$ at $k = k_{\rm A} := 0.6$ and $k = k_{\rm B} := 2.0$, respectively, which correspond to the cross symbols in Fig. 4. The upper sides denote symmetric connection delays $\tau = \tau^*$ and the lower sides denote asymmetric connection delays (18). All of the oscillators are uncoupled until $t = 50$ and are then coupled at $t = 50$. The variables quench (i.e., the occurrence of AD) at $k = k_{\rm A}$ for both symmetric and asymmetric connection delays, but still oscillate at $k = k_{\rm B}$ as shown in Fig. 5(b)[5].

3.2 Cyclic graph

This subsection deals with networks having a cyclic graph, which has a cyclic path, and that are not covered by Theorem 1. Let us consider the networks shown in Fig. 6. Both networks shown in Figs. 6(b) and 6(c) satisfy Eq. (15) with $\tau = 5$. Figure 7 shows the largest real part of roots of $g(s) = 0$ for the networks of Fig. 6 with varying coupling strength k. The networks in Figs. 6(a) and 6(b) have different real parts. Note that, for the network in Fig. 6(a), $g(s)$ is unstable for any k, whereas for the network of Figs. 6(b), $g(s)$ is stable for the range of $k \in (0.37, 2.70)$. Therefore, if the network topology includes a cyclic graph, the stability of steady state (3) with asymmetric connection delays is not always same as that with symmetric connection delays, even when Eq. (15) is satisfied.

On the other hand, interestingly, the largest real part for the networks of Figs. 6(a) and 6(c) are exactly same, i.e., they have the same stability of steady state (3) although the network topology is not a tree graph. Here, we briefly discuss the reason for this. Let $\{o_1, o_2, \ldots, o_n\}$ be the directed path from oscillator o_1 to oscillator o_n ($o_i \in \{1, \ldots, N\}$). For the network in Fig. 6(c), the sum of the connection delays in a closed path $\{2, 3, 4, 2\}$ is equal to that in the closed path of the counter direction, i.e., $\tau_{32} + \tau_{43} + \tau_{24} = 15$ and $\tau_{42} + \tau_{34} + \tau_{23} = 15$. Note that this relation holds for symmetric connection delays (i.e., the network in Fig. 6(a)). In contrast, for the network in Fig. 6(b), the sum of connection delays in the path $\{2, 3, 4, 2\}$ is 22.8, and that in the counter direction is 7.2. This difference would cause the stability to differ for the networks in Figs. 6(b) and 6(c) and to be the same for the networks in Figs. 6(a) and 6(c). Furthermore, we have

[5] For symmetric connection delays, all of the variables converge to the synchronized state $\boldsymbol{s}(t) := \boldsymbol{x}_1(t) = \cdots = \boldsymbol{x}_N(t)$. For asymmetric connection delays, a synchronized state cannot be described by $\boldsymbol{s}(t)$ due to the asymmetricity; thus, the variables do not converge to $\boldsymbol{s}(t)$.

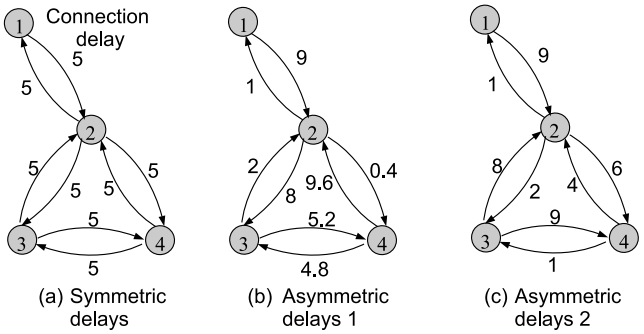

Fig. 6. Cycle graph ($N = 4$)

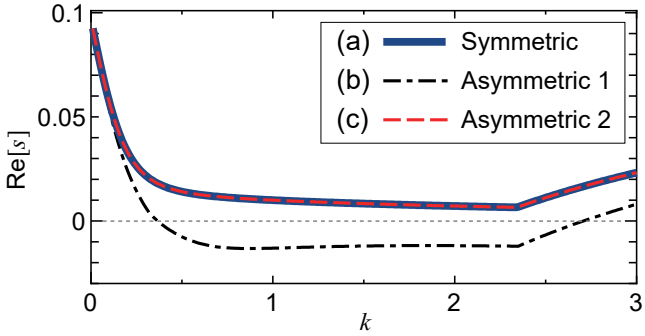

Fig. 7. Largest real part of roots for the networks shown in Fig. 6

numerically confirmed that the above consideration can be also observed for the following two networks: an $N = 6$ oscillators network with two cycles and an $N = 9$ oscillators network with three cycles. The analytical proof of this consideration in general networks is our future task.

4 Conclusion

The present study investigated AD in asymmetric delayed-coupled oscillators with a tree graph topology. We found that the stability depends on the sum of the connection delays between connected oscillators. Therefore, we reported that the stability of the steady state with asymmetric connection delays can be reduced to that with symmetric connection delays if the sums of the connection delays between connected oscillators are identical. The analytical results were confirmed through numerical simulations.

A Proof of Lemma 1

This proof uses the following information regarding a tree graph:

(i) Every tree with two or more nodes has at least two nodes of degree one (Corollary 2.2 in [31]);
(ii) A subgraph of a tree is a forest[6] (Remarks 4.2.1 in [32]);

[6] A forest is a graph without cycles.

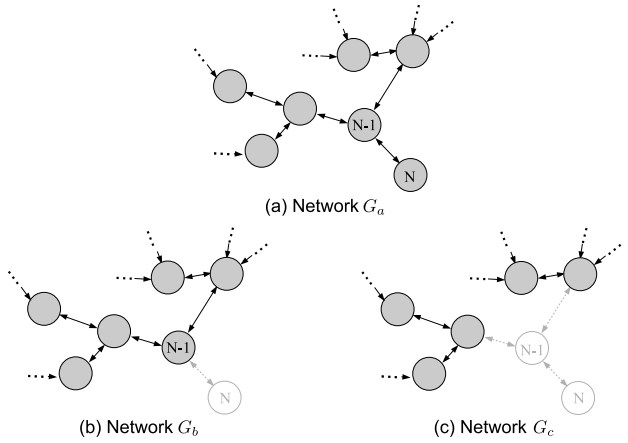

Fig. 8. Sketches of networks G_a, G_b, and G_c

(iii) Each component of a forest is a tree [32].

From fact (i), a tree with $N \geq 2$ always has a node of degree one. Without loss of generality, let oscillator N be an oscillator of degree one, which is connected only to oscillator $(N-1)$ (see Fig. 8(a)). This network is referred hereinafter to as network G_a. Then, the matrix $\hat{\boldsymbol{E}}(s) := \boldsymbol{I}_N - \hat{G}(s)\boldsymbol{E}(s)$ in Eq. (14) is rewritten as[7]

$$\hat{\boldsymbol{E}}(s) = \left[\begin{array}{ccc|cc} & \boldsymbol{E}_c(s) & & \{\hat{\boldsymbol{E}}(s)\}_{1,N-1} & 0 \\ & & & \vdots & \vdots \\ & & & \{\hat{\boldsymbol{E}}(s)\}_{N-2,N-1} & 0 \\ \hline \{\hat{\boldsymbol{E}}(s)\}_{N-1,1} & \cdots & \{\hat{\boldsymbol{E}}(s)\}_{N-1,N-2} & 1 & \{\hat{\boldsymbol{E}}(s)\}_{N-1,N} \\ 0 & \cdots & 0 & \{\hat{\boldsymbol{E}}(s)\}_{N,N-1} & 1 \end{array}\right], \quad (19)$$

where $\boldsymbol{E}_c(s)$ is the $(N-2)\times(N-2)$ upper-left submatrix of the matrix $\hat{\boldsymbol{E}}(s)$. Since the degree of oscillator N is one, all of the elements in the Nth row (column) of matrix (19) are zero, except for $\{\hat{\boldsymbol{E}}(s)\}_{N,N-1}$ ($\{\hat{\boldsymbol{E}}(s)\}_{N-1,N}$) and $\{\hat{\boldsymbol{E}}(s)\}_{N,N} = 1$.

Expanding $\hat{g}(s)$ along the Nth row of $\hat{\boldsymbol{E}}(s)$ yields

$$\hat{g}(s) = \det\boldsymbol{E}_b(s) - \{\hat{\boldsymbol{E}}(s)\}_{N,N-1} \cdot \det\left[\begin{array}{ccc|c} & \boldsymbol{E}_c(s) & & 0 \\ & & & \vdots \\ & & & 0 \\ \hline \{\hat{\boldsymbol{E}}(s)\}_{N-1,1} & \cdots & \{\hat{\boldsymbol{E}}(s)\}_{N-1,N-2} & \{\hat{\boldsymbol{E}}(s)\}_{N-1,N} \end{array}\right], \quad (20)$$

$$\boldsymbol{E}_b(s) := \left[\begin{array}{ccc|c} & \boldsymbol{E}_c(s) & & \{\hat{\boldsymbol{E}}(s)\}_{1,N-1} \\ & & & \vdots \\ & & & \{\hat{\boldsymbol{E}}(s)\}_{N-2,N-1} \\ \hline \{\hat{\boldsymbol{E}}(s)\}_{N-1,1} & \cdots & \{\hat{\boldsymbol{E}}(s)\}_{N-1,N-2} & 1 \end{array}\right]. \quad (21)$$

[7] Since $D_g(s) + kN_g(s)$ in Eq. (13) does not depend on the network topology or connection delays, we consider only $\hat{g}(s) := \det\hat{\boldsymbol{E}}(s)$ in Eq. (14).

Furthermore, expanding the determinant of the 2nd term in Eq. (20) along the $(N-1)$th column, we have

$$\begin{aligned}\hat{g}(s) &= \det\boldsymbol{E}_b(s) - \{\hat{\boldsymbol{E}}(s)\}_{N,N-1}\{\hat{\boldsymbol{E}}(s)\}_{N-1,N}\det\boldsymbol{E}_c(s) \\ &= \det\boldsymbol{E}_b(s) - \frac{\hat{G}^2(s)}{d_N d_{N-1}} e^{-s\left(\tau_{N(N-1)}+\tau_{(N-1)N}\right)}\det\boldsymbol{E}_c(s). \end{aligned} \quad (22)$$

Let us focus on $\det\boldsymbol{E}_b(s)$ and $\det\boldsymbol{E}_c(s)$ in Eq. (22). From Eqs. (19) and (21), we see that $\det\boldsymbol{E}_b(s)$ corresponds to a characteristic quasi-polynomial for network G_b, which is constructed by removing oscillator N from network G_a (see Fig. 8(b)). In the same manner, $\det\boldsymbol{E}_c(s)$ corresponds to a characteristic quasi-polynomial for network G_c which is constructed by removing oscillators N and $(N-1)$ from network G_a (see Fig. 8(c)). Note that both networks G_b and G_c are subgraphs of G_a. Thus, based on (ii) and (iii), the networks are forests, and their components are trees. In addition, the second term of Eq. (22) contains the sum of connection delays between the oscillator of degree one and the oscillator connected to the previous oscillator in network G_a [i.e., $(\tau_{N(N-1)} + \tau_{(N-1)N})$].

As a consequence, by expanding a quasi-polynomial of a network with a tree graph (i.e., $\det\hat{\boldsymbol{E}}(s)$) along an oscillator of degree one, we obtain the two characteristic quasi-polynomials (i.e., $\det\boldsymbol{E}_b(s)$ and $\det\boldsymbol{E}_c(s)$). Since these characteristic quasi-polynomials correspond to networks whose components are tree graphs, they can be expanded by focusing on an oscillator of degree one. Furthermore, expanding the characteristic quasi-polynomials yields the sum of connection delays between an oscillator of degree one and an oscillator connected to the previous oscillator in the exponent (see Eq. (22)). As a consequence, by repeating the expansion, we obtain the sum of the connection delays between all connected oscillators. Therefore, we can recursively prove that the stability of steady state (3) depends on the sum of the connection delays between connected oscillators. □

Acknowledgments

The present study was supported in part by JSPS KAKENHI (17K12748).

Author contribution statement

Y. Okigawa and Y. Sugitani performed analytical calculations and numerical simulations. K. Konishi and Y. Sugitani wrote the manuscript.

References

1. G. Saxena, A. Prasad, R. Ramaswamy, Phys. Rep. **521**, 205 (2012)
2. A. Koseska, E. Volkov, J. Kurths, Phys. Rep. **531**, 173 (2013)

3. A. Koseska, E. Volkov, J. Kurths, Phys. Rev. Lett. **111**, 024103 (2013)
4. D.G. Aronson, G.B. Ermentrout, N. Kopell, Physica D **41**, 403 (1990)
5. D.V. Reddy, A. Sen, G.L. Johnston, Phys. Rev. Lett. **80**, 5109 (1998)
6. D.V. Reddy, A. Sen, G.L. Johnston, Physica D **129**, 15 (1999)
7. F.M. Atay, Phys. Rev. Lett. **91**, 094101 (2003)
8. Y. Sugitani, K. Konishi, L.B. Le, N. Hara, Chaos **24**, 043105 (2014)
9. K. Suresh, S. Sabarathinam, K. Thamilmaran, J. Kurths, S.K. Dana, Chaos **26**, 083104 (2016)
10. S.R. Huddy, J. Sun, Phys. Rev. E **93**, 052209 (2016)
11. C. Yao, Q. Zhao, W. Zou, Eur. Phys. J. B **89**, 29 (2016)
12. R.M. Nguimdo, Phys. Rev. E **97**, 032211 (2018)
13. N. Zhao, Z. Sun, W. Xu, Eur. Phys. J. B **91**, 20 (2018)
14. K. Manoj, S.A. Pawar, R.I. Sujith, Sci. Rep. **8**, 11626 (2018)
15. R.A. Van Gorder, A.L. Krause, J.A. Kwiecinski, Nonlinear Dyn. **97**, 151 (2019)
16. A. Sharma, Phys. Lett. A **383**, 1865 (2019)
17. R. Xiao, Z. Sun, X. Yang, W. Xu, Nonlinear Dyn. **95**, 2093 (2019)
18. S. Roy Choudhury, D. Mandragona, Int. J. Bifurcat. Chaos **29**, 1950019 (2019)
19. D.Q. Wei, B. Zhang, X.S. Luo, S.Y. Zeng, D.Y. Qiu, IEEE Trans. Circuits Syst., II, Exp. Briefs **60**, 692 (2013)
20. T. Biwa, S. Tozuka, T. Yazaki, Phys. Rev. Applied **3**, 034006 (2015)
21. S.R. Huddy, J.D. Skufca, IEEE Trans. Power Electron. **28**, 247 (2013)
22. H. Hyodo, T. Biwa, Phys. Rev. E **98**, 052223 (2018)
23. N. Thomas, S. Mondal, S.A. Pawar, R.I. Sujith, Chaos **28**, 093116 (2018)
24. H. Jegal, K. Moon, J. Gu, L.K.B. Li, K.T. Kim, Combust. Flame **206**, 424 (2019)
25. S.H. Strogatz, Nature **394**, 316 (1998)
26. C. Cakan, J. Lehnert, E. Schöll, Eur. Phys. J. B **87**, 54 (2014)
27. M. Ponce, C. Masoller, A.C. Martí, Eur. Phys. J. B **67**, 83 (2009)
28. N. Punetha, R. Karnatak, A. Prasad, J. Kurths, R. Ramaswamy, Phys. Rev. E **85**, 046204 (2012)
29. F.M. Atay, J. Differ. Equ. **221**, 190 (2006)
30. K. Konishi, Phys. Lett. A **341**, 401 (2005)
31. J.A. Bondy, U.S.R. Murty, *Graph theory with applications* (Elsevier Science Ltd, 1976)
32. R. Balakrishnan, K. Ranganathan, *A textbook of graph theory* (Springer, 2012)